Molecular profiling of single circulating tumor cells from lung cancer patients

Seung-min Park[a,b,1], Dawson J. Wong[c,1], Chin Chun Ooi[d,1], David M. Kurtz[b,e,f], Ophir Vermesh[a,b], Amin Aalipour[a,b], Susie Suh[g], Kelsey L. Pian[h], Jacob J. Chabon[i], Sang Hun Lee[j], Mehran Jamali[a], Carmen Say[k], Justin N. Carter[k], Luke P. Lee[j], Ware G. Kuschner[l,m], Erich J. Schwartz[n], Joseph B. Shrager[o], Joel W. Neal[f,p], Heather A. Wakelee[f,p], Maximilian Diehn[i,k,p,q], Viswam S. Nair[a,m,q,2], Shan X. Wang[c,h,q,2], and Sanjiv S. Gambhir[a,b,q,2]

[a]Department of Radiology, Stanford University School of Medicine, Stanford, CA 94305; [b]Molecular Imaging Program at Stanford, Stanford University School of Medicine, Stanford, CA 94305; [c]Department of Electrical Engineering, Stanford University, Stanford, CA 94305; [d]Department of Chemical Engineering, Stanford University, Stanford, CA 94305; [e]Department of Bioengineering, Stanford University, Stanford, CA 94305; [f]Division of Oncology, Department of Medicine, Stanford University School of Medicine, Stanford, CA 94305; [g]Department of Pharmacology, Case Western Reserve University School of Medicine, Cleveland, OH 44106; [h]Department of Materials Science and Engineering, Stanford University, Stanford, CA 94305; [i]Institute for Stem Cell Biology and Regenerative Medicine, Stanford University School of Medicine, Stanford, CA 94305; [j]Department of Bioengineering, University of California, Berkeley, CA 94720; [k]Department of Radiation Oncology, Stanford University School of Medicine, Stanford, CA 94305; [l]Section of Pulmonary and Critical Care Medicine, Veterans Affairs Palo Alto Health Care System, Palo Alto, CA 94304; [m]Division of Pulmonary and Critical Care Medicine, Department of Medicine, Stanford University School of Medicine, Stanford, CA 94305; [n]Department of Pathology, Stanford University School of Medicine, Stanford, CA 94305; [o]Department of Cardiothoracic Surgery, Stanford University School of Medicine, Stanford, CA 94305; [p]Stanford Cancer Institute, Stanford University School of Medicine, Stanford, CA 94305; and [q]Canary Center at Stanford for Cancer Early Detection, Stanford University School of Medicine, Palo Alto, CA 94305

Edited by John A. Rogers, University of Illinois, Urbana, IL, and approved October 28, 2016 (received for review May 27, 2016)

Circulating tumor cells (CTCs) are established cancer biomarkers for the "liquid biopsy" of tumors. Molecular analysis of single CTCs, which recapitulate primary and metastatic tumor biology, remains challenging because current platforms have limited throughput, are expensive, and are not easily translatable to the clinic. Here, we report a massively parallel, multigene-profiling nanoplatform to compartmentalize and analyze hundreds of single CTCs. After high-efficiency magnetic collection of CTC from blood, a single-cell nanowell array performs CTC mutation profiling using modular gene panels. Using this approach, we demonstrated multigene expression profiling of individual CTCs from non–small-cell lung cancer (NSCLC) patients with remarkable sensitivity. Thus, we report a high-throughput, multiplexed strategy for single-cell mutation profiling of individual lung cancer CTCs toward minimally invasive cancer therapy prediction and disease monitoring.

circulating tumor cells | microfluidics | rare-cell sorting | reverse transcription-PCR | single-cell analysis

Blood-based biomarkers, including genomic, transcriptomic, proteomic, and other cellular components, are amenable to minimally invasive approaches for cancer detection and assessment (1). Circulating tumor cells (CTCs), which are currently defined as epithelial cells in a cancer patient's bloodstream derived from tumor cell release, are an established prognostic blood biomarker, because their concentration in blood is associated with high tumor burden (2). CTC gene expression and gene mutation profiling may therefore noninvasively recapitulate the primary and metastatic tumor composition, potentially yielding clinically actionable information. Therefore, CTC single-cell mutation analysis for clinical application may be a practical approach for tumor progression monitoring and treatment selection.

CellSearch is the only US Food and Drug Administration-approved technology since its introduction in 1999 to identify CTCs in whole blood (3). Many other innovative platforms (2) leverage various physical and biochemical properties of CTCs for highly sensitive and efficient enrichment (2), encompassing improved epithelial cell adhesion molecule (EpCAM)-based capture [e.g., CTC Chip (4), HB-Chip (5), μNMR (6), MagSweeper (7), and MagSifter (8)], size-selective capture [e.g., Cluster-Chip (9), ISET (2, 10), and Vortex technologies (11)], inertial-based capture [e.g., iChip platform (12)], nanomaterials-based capture [e.g., nanofilms (13), NanoVelcro (14), and functionalized graphene oxide nanosheets (15)], and image-based cytometry [e.g., HD-CTC (16)].

These current platforms, unfortunately, are overwhelmingly reliant on the enumeration of CTCs by immunocytochemistry (ICC) to measure tumor burden, which clearly does not probe underlying CTC tumor biology. To overcome limitations of existing CTC identification strategies, downstream analysis of individual CTCs via highly sensitive and specific single-cell measurements of tumor-derived blood components is imperative. Investigators have detected CTCs via gene expression directly from unprocessed whole blood (17, 18), but these measurements are typically (*i*) obscured by background signals from circulating mRNA, white blood cells (WBCs), and other blood components (19) and (*ii*) performed using ensemble measurements that inadequately represent individual cell phenotypes. Because this analysis averages out signals across individual CTCs, the heterogeneity of different CTC populations is not detected, which could play a critical role in understanding a patient's tumor biology, metastatic potential, and

Significance

There exists an urgent need for minimally invasive molecular analysis tools for cancer assessment and management, particularly in advanced-stage lung cancer, when tissue procurement is challenging and gene mutation profiling is crucial to identify molecularly targeted agents for treatment. High-throughput compartmentalization and multigene profiling of individual circulating tumor cells (CTCs) from whole-blood samples using modular gene panels may facilitate highly sensitive, yet minimally invasive characterization of lung cancer for therapy prediction and monitoring. We envision this nanoplatform as a compelling research tool to investigate the dynamics of cancer disease processes, as well as a viable clinical platform for minimally invasive yet comprehensive cancer assessment.

Author contributions: S.-m.P., D.J.W., C.C.O., D.M.K., O.V., S.H.L., L.P.L., M.D., V.S.N., S.X.W., and S.S.G. designed research; S.-m.P., D.J.W., C.C.O., S.S., K.L.P., and S.S.G. performed research; S.-m.P., D.J.W., C.C.O., D.M.K., O.V., A.A., S.S., J.J.C., M.J., C.S., J.N.C., W.G.K., J.B.S., J.W.N., H.A.W., M.D., V.S.N., S.X.W., and S.S.G. contributed new reagents/analytic tools; S.-m.P., D.J.W., C.C.O., O.V., A.A., S.S., K.L.P., J.J.C., E.J.S., M.D., V.S.N., S.X.W., and S.S.G. analyzed data; and S.-m.P., D.J.W., C.C.O., V.S.N., S.X.W., and S.S.G. wrote the paper.

Conflict of interest statement: S.X.W. holds two issued patents on MagSifter, which are owned by Stanford University and outlicensed for possible commercialization. S.-m.P., D.J.W., C.C.O., S.S.G., V.S.N., and S.X.W. are coinventors of a pending patent filed by Stanford University on the subject of this work.

This article is a PNAS Direct Submission.

[1]S.-m.P., D.J.W., and C.C.O. contributed equally to this work.

[2]To whom correspondence may be addressed. Email: sgambhir@stanford.edu, viswamnair@stanford.edu, or sxwang@stanford.edu.

This article contains supporting information online at www.pnas.org/lookup/suppl/doi:10.1073/pnas.1608461113/-/DCSupplemental.

clinical course (20). Other reported methods for single-cell multigene expression CTC profiling of breast cancer (21) and metastatic prostate cancer (22) suffer from limited throughput—each captured cell is manually selected, lysed, and subjected to reverse transcription into cDNA before parallel multigene expression profiling, thus precluding their large-scale clinical application.

In particular, lung cancer presents an urgent need for a routine, minimally invasive clinical assessment tool, because (*i*) it is the leading cause of cancer deaths worldwide (23); (*ii*) many lung cancer patients are diagnosed at the most advanced stage; (*iii*) new molecularly targeted therapies are emerging to improve progression-free and overall survival for those patients with driver mutations such as epidermal growth factor receptor (EGFR) (24) and anaplastic lymphoma kinase (ALK) (25); (*iv*) new methods for diagnosis and treatment monitoring are imperative because accessing the primary tumor or metastatic lesions can be technically challenging, morbid, and costly; and (*v*) CTCs have been isolated and profiled for key driver mutations in non–small-cell lung cancer (NSCLC) (17).

With the above needs in mind, we report the development, validation, and demonstrated clinical utility of an integrated nanoplatform that features a magnetic sifter [MagSifter (8)] and single-cell nanowell array capable of sorting up to 25,600 cells [Nanowell (26, 27)] to capture, easily compartmentalize, and molecularly characterize single CTCs from blood (Fig. 1). We report here a proof-of-concept demonstration showing single-CTC multigene expression and mutation profiling for tumor interrogation using four-plex modular gene panels, including panels for EGFR mutation detection for therapy prediction and monitoring.

Results

Overall Workflow. The Nanowell performs massively parallel sorting of individual CTCs into 25,600 separate compartments. First, the MagSifter technology (8) (Fig. 1 and Fig. S1) tags CTCs with magnetic nanoparticles for high-throughput, high-efficiency CTC enrichment from blood. After MagSifter enrichment from 2-mL whole-blood samples (see Fig. S2 for illustration of captured cells via conventional ICC), red blood cells (RBCs) are hemolyzed (28) and DNase I is added to remove circulating genomic DNA, obtaining ultrapure cellular eluent that is seeded into Nanowell by direct pipetting and centrifugation. Single-cell multigene RT-PCR is performed with our modular multigene panels: a CTC identification panel with telomerase reverse transcriptase (*TERT*) (29, 30) and mesenchymal–epithelial transition (*MET*) (31, 32) to identify putative CTCs in advanced-stage NSCLC patients, and a therapy prediction and monitoring panel with *TERT*, an EGFR mutation, and its corresponding wild-type gene for identification and mutation detection of putative CTCs in advanced-stage NSCLC. NSCLC and noncancer cell lines were used to validate the gene expression panels on the integrated nanoplatform. To demonstrate its potential for clinical translation, samples from both healthy human subjects and patients diagnosed with NSCLC with the CTC identification panel (*TERT* and *MET*) were assayed.

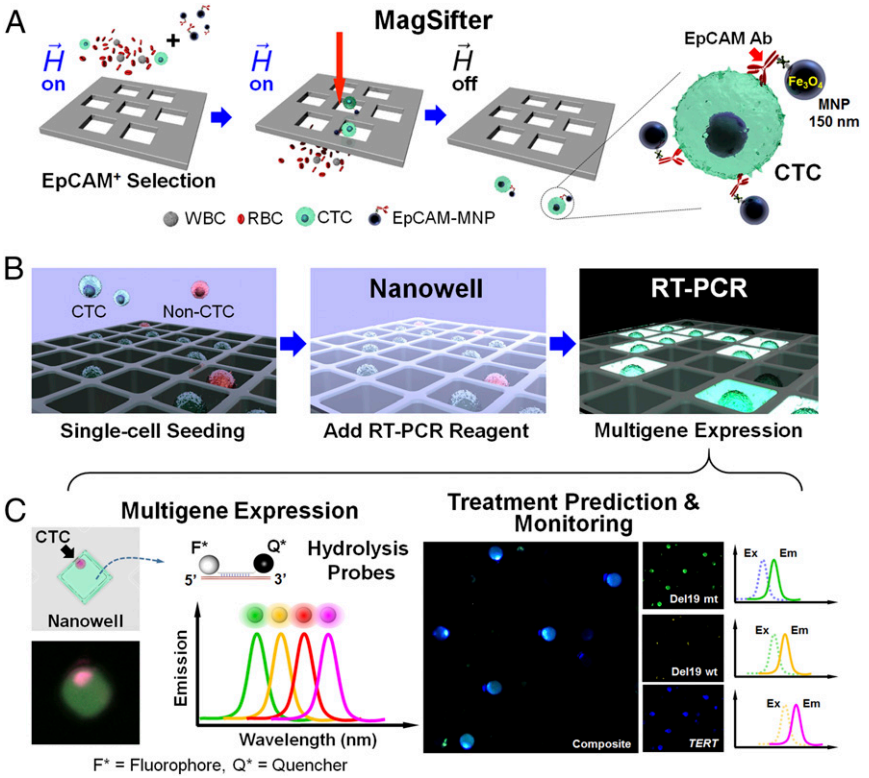

Fig. 1. Overall workflow of the integrated nanoplatform. (*A*) First, whole-blood samples are processed for isolation of CTCs by the MagSifter. Streptavidinated 150-nm iron oxide magnetic nanoparticles (MNPs) are conjugated to biotinylated anti-EpCAM antibodies for EpCAM-positive selection of circulating tumor cells (CTCs), which are epithelial in origin. Magnetically labeled CTCs are captured on the sifter when flowed through it under an applied magnetic field and subsequently eluted in the absence of a magnetic field. (*B*) Subsequently, all eluent is directly loaded without staining onto a Nanowell device, and cells are seeded into individual compartments by centrifugation. After drying, single-cell RT-PCR mix is applied to the nanowells, which are then sealed with PCR tape. (*C*) The Nanowell device is then placed into a thermocycler for multiplex gene mutation and expression analysis via reverse transcription and PCR amplification. Multigene expression via up to four off-the-shelf hydrolysis probes with discrete emission spectra can be imaged in each nanowell. These fluorescence signals are then analyzed with custom MATLAB and R scripts for identification and characterization of putative CTCs based on modular panels of representative genes. These panels are flexible and can be adjusted to accommodate clinical needs such as therapy prediction and disease monitoring.

Then, therapy prediction and monitoring (*TERT*, EGFR mutant, and EGFR wild-type) panels were assayed using advanced-stage NSCLC patient blood samples.

Single-Cancer-Cell Detection Using the Nanowell Assay on Cell Lines. We first identified mutations in HCC827 and H661 cell lines (Fig. 2*A*), which are mutant and wild type, respectively, for EGFR exon 19 deletion (del19) in bulk and then at the individual-cell level to demonstrate the utility of Nanowell. Bulk gene expression analysis of total mRNA extracted from 10^6 cells each of HCC827 and H661 indicated their mutually exclusive gene expression of EGFR E746-A750del [the most common del19 mutation (33)] and wild type, respectively ($P < 0.0001$, two-sample t test). Nanowell confirmed differential del19 expression between HCC827 and H661, with individual HCC827 cells expressing only EGFR E746-A750del (green) and individual H661 cells exhibiting only wild-type EGFR (orange) ($P < 0.0001$) (Fig. 2*B*).

We further examined the bulk gene expression of 10^6 cells each of five NSCLC cell lines (A549, H661, H1650, H1975, and HCC827), a noncancerous fibroblast (PCS-201) cell line, and WBCs from 2 mL of healthy human blood. Cancer cells expressed significantly higher *TERT* and *MET* than PCS-201 cells and WBCs ($P < 0.0001$, t test), both of which expressed no *TERT* and low *MET* (Fig. 2*C*), thus implying that *TERT* and *MET* are good CTC markers.

We then assessed Nanowell's ability to distinguish between cancerous and noncancerous cells by differential gene expression profiling of H1650 and PCS-201 cell lines. H1650 and PCS-201 cells were stained with CellTracker Green CMFDA and Orange CMRA dyes (Life Technologies), respectively, and assayed together in a Nanowell for *TERT*. Nanowell images were acquired in three fluorescence channels corresponding to H1650 cells (as denoted in green color), PCS-201 cells (denoted as red color), and *TERT* gene expression (denoted as blue color) (Fig. 2*D*). *TERT* expression signals revealed a significant differentiation between H1650 and PCS-201 cells ($P < 0.0001$, t test).

Four-Plex Gene Expression of Single H1650 Cells Spiked into Healthy Blood. To validate the suitability of a modular gene panel including vimentin (*VIM*) and aldehyde dehydrogenase (*ALDH*) in addition to *TERT* and *MET* for CTC identification, we examined the bulk gene expression of 10^6 cells from each of five NSCLC cell lines (A549, H661, H1650, H1975, and HCC827), a noncancerous fibroblast (PCS-201) cell line, and WBCs from 2 mL of healthy human blood. We noted heterogeneous *VIM* and *ALDH* expression across these cell types (Fig. S3).

After performing these in vitro experiments, we assessed whether our platform could isolate cells spiked into healthy human blood using H1650 cells, which mimics the NSCLC patient condition (Fig. 3*A*). After demonstrating bulk gene expression for our four-plex assay *TERT*, *MET*, *VIM*, and *ALDH*, we observed distinct patterns of gene expression on individual cells isolated from doped blood (Fig. 3*B*). One cell population

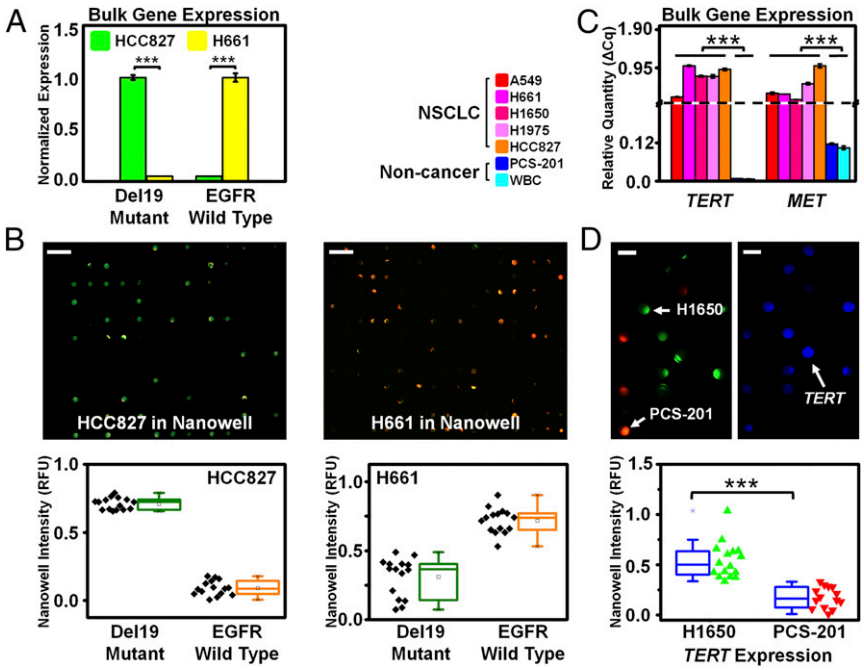

Fig. 2. Translating bulk gene expression to single-cell gene expression profiling on Nanowell using cell lines. (*A*) Two cell lines (HCC827 and H661) were selected according to their EGFR exon 19 deletion (del19) mutational status (mutant and wild type, respectively). Bulk expression analysis by PCR showed that HCC827 cells exhibited measured signal for only the EGFR E746-A750del (the most common EGFR del19 mutation shown in green), with undetectable wild-type EGFR. In contrast, H661 cells exhibited measured signal for only the wild-type EGFR shown in yellow, with undetectable E746-A750del. (*B*) The same two cell lines each underwent single-cell analysis on Nanowell using EGFR E746-A750del and wild-type probes in FAM (shown in green) and HEX (shown in orange) channels, respectively. HCC827 cells exhibited fluorescence predominantly in the FAM channel, indicating the presence of EGFR del19 mutation. (Scale bar, 200 μm.) In contrast, the assay of H661 cells exhibited fluorescence predominantly in the HEX channel, indicating the presence of wild-type EGFR. (Scale bar, 200 μm.) For each cell line, we observed a clear differentiation between the EGFR mutant and wild-type expression levels from single cells in Nanowell, and the bulk expression measurements matched the corresponding Nanowell signal, with high statistical significance ($P < 0.0001$ for both cases, t test). (*C*) Bulk gene expression among five NSCLC cell lines (A549, H661, H1650, H1975, and HCC827), a noncancerous fibroblast cell line (PCS-201), and WBCs are shown by quantitative RT-PCR. The five cancer cell lines exhibited high *TERT* and *MET* gene expression, whereas the fibroblast cells and WBCs exhibited no *TERT* and low *MET* expression. (*D*) Single-cell analysis using Nanowell on cancer and noncancer populations by RT-PCR expression analysis on H1650 and PCS-201 cell lines. (Scale bar, 50 μm.) Each cell line was stained with different CellTracker dyes (green for H1650; orange for PCS-201) and then imaged to illustrate the concordance between each cell's Nanowell location and RT-PCR signal (*TERT* shown in blue). Nanowell showed a clear differentiation between H1650 (cancer; $n = 16$) and PCS-201 (noncancer; $n = 14$) cell lines based on *TERT* expression, with high statistical significance ($P < 0.0001$, t test).

expressed high *VIM* only (Fig. 3 *C*, *E*, and *F*), which we attribute to WBCs' mesenchymal cell origin (34), whereas the second cell population expressed high *TERT*, *MET*, and *VIM*, and variable *ALDH* (Fig. 3 *D*–*F*), corresponding to H1650s bulk expression. Importantly, these single-cell observations matched our bulk analysis from Fig. 2 and Fig. S3. Quantitative analysis of total gene expression, normalized by H1650 expression, indicated differential *TERT* and *MET* expression in WBCs and H1650 cells ($P < 0.0001$ for both cases, *t* test), indicating *TERT* and *MET* are both excellent markers to identify cancer cells compared with WBCs (Fig. 3*E*). Average *VIM* and *ALDH* expression was similar between H1650 cells and WBCs, and H1650 expressed *ALDH* with higher variance (Fig. 3*F*).

Multiplex Gene Expression Analysis of CTCs in NSCLC Cancer Patients. Following a successful demonstration of multiplexed gene profiling of individual cancer cells from cell lines in spiked blood, we proceeded to analyze whole-blood samples from 55 human subjects (from June 2014 to August 2016). We analyzed blood from 20 healthy individuals from the Stanford Blood Center and 35 patients with stage IV NSCLC of adenocarcinoma histology to first identify CTCs by single-cell *TERT* and *MET* expression profiling, and second to determine whether these putative CTCs were abundant in NSCLC and not in healthy patients (Fig. 3 *G* and *H* and Table S1).

A representative stage IV Nanowell scan revealed a substantial number of nanowells with positive *TERT* and *MET* signal from single putative CTCs, whereas the healthy donor Nanowell exhibited negligible signals (Fig. 3*G*). Putative CTCs were detected in almost all advanced-stage NSCLC samples, from 0 to 181 [interquartile range (IQR), 10–30] (Fig. 3*H*). In contrast, up to 7 positive wells out of 25,600 were detected in healthy controls (IQR, 2–6). Considering 7 or more putative CTCs in 2 mL as a positive sample, we detected putative CTCs in 31 of 35 (88.6%) patients. Because CellSearch detects clinically meaningful levels of CTCs in just 53% of patients with advanced-stage NSCLC (35), our platform demonstrated higher capability to identify putative CTCs.

Interestingly, a stage III NSCLC patient blood sample revealed heterogeneity of expression across putative CTCs (Fig. 3*I*). From each cell's multigene expression profile, a clear differentiation between putative CTCs and WBCs emerged, as predicted from the spike-in cell line experiments. Putative CTCs were identified by their high expression of both *TERT* and *MET*, whereas WBCs were identified by nanowells lacking *TERT* and

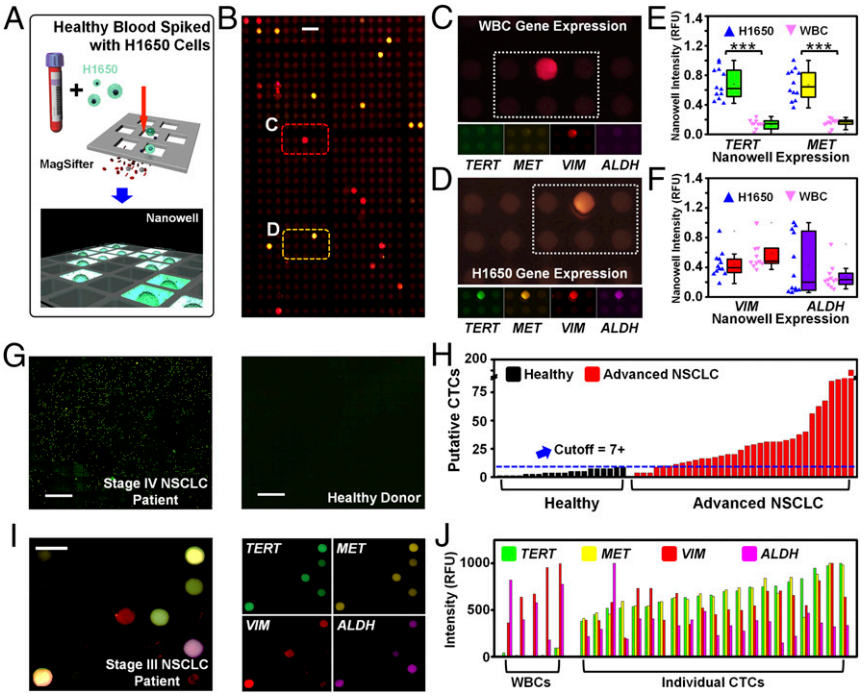

Fig. 3. Validation of our integrated nanoplatform with blood samples. (*A*) Workflow schematic of validation experiments. H1650 cells were spiked into whole-blood samples from healthy human subjects and processed through the MagSifter and Nanowell. (*B*) Scanned fluorescence images on Nanowell after RT-PCR amplification of four genes on the spike-in cells recovered using MagSifter. (Scale bar, 50 μm.) These genes were selected to identify putative CTCs (*TERT* and *MET*) and to demonstrate the multiplex capability of the assay using biologically informative targets (*VIM* and *ALDH*). Two major populations were visually observed: one with a primarily red color (*C*) and another with a primarily yellow color (*D*). (*C*) This cell population primarily expressed *VIM* and none of the other three assayed genes, which is characteristic of leukocytes (WBCs). (*D*) In contrast, a second cell population expressed *TERT*, *MET*, and *VIM*, and partially expressed *ALDH*, which is characteristic of H1650 cancer cells. (*E*) Quantitative analysis of Nanowell after RT-PCR exhibited a clear differentiation of *TERT* and *MET* expression levels between the cell populations in *C* and *D* (nominally WBCs and H1650 cells), with high statistical significance ($P < 0.0001$ for both cases, *t* test). (*F*) Quantitative analysis of *VIM* and *ALDH* expression revealed similar *VIM* expression between the two cell populations, whereas the *ALDH* expression in the latter cell population exhibited higher variance. (*G*) A two-channel fluorescence composite scan of the entire Nanowell array (25,600 wells) after on-chip RT-PCR using *TERT* and *MET* probes shows a stage IV NSCLC patient sample (*Left*), with a substantial number of *TERT* and *MET* positive wells. In contrast, the similar scan of a healthy donor blood sample (*Right*) lacked *TERT* and *MET* signal. (Scale bar, 1,000 μm.) (*H*) The MagSifter and Nanowell were used for CTC identification in blood samples (defined as the population of $EpCAM^+$ cells with expression of both *TERT* and *MET* in a nanowell). Our 55 assayed samples consisted of 35 advanced-stage NSCLC samples and 20 healthy control samples. (*I*) Multigene expression of CTCs from NSCLC patient blood. A representative portion of the fluorescence scan (superimposed in four channels) of a completed Nanowell multigene expression panel for a stage III NSCLC patient sample displayed heterogeneous single-cell gene expression across nanowells. (Scale bar, 50 μm.) (*J*) A quantitative representation of the four-plex data confirmed that putative CTCs exhibit high *TERT* and *MET* expression and variable *VIM* and *ALDH* expression. In contrast, WBCs exhibit high *VIM* expression, variable *ALDH* expression, and low *TERT* and *MET* expression.

MET expression and exhibiting high *VIM* expression. Variable *VIM* and *ALDH* expression was observed for putative CTCs (Fig. 3*J*), which may reflect the heterogeneity of CTC populations present in lung cancer patients (36, 37).

EGFR Mutation Detection in Single CTCs from NSCLC Patients. We then used our integrated nanoplatform to detect the most common and clinically relevant EGFR mutations (del19, L858R, and T790M) in CTCs from seven stage IV NSCLC adenocarcinoma patients who had known EGFR mutation status confirmed by tumor biopsy. Putative CTCs were assessed for three genes: *TERT*, the EGFR mutation (E746-A750del, L858R, or T790M), and the corresponding EGFR wild type (Fig. 4). Because *TERT* gene exhibits superior distinction on cancer cell identification (Fig. 2), putative CTCs were identified by high *TERT* expression. Notably, we were able to accurately detect each patient's known mutation from their putative CTCs (Fig. 4 *B*, *D*, and *F*), whereas the "bulk" RT-qPCR measurements from the same patient's blood yielded undetectable levels of the assayed genes (Fig. 4 *B* and *D*). Putative CTCs from E746-A750del visually appeared green (indicative of the EGFR mutation), whereas yellow (EGFR wild type) was nearly absent (Fig. 4*A*). Quantitative analysis of putative CTCs confirmed that the majority of these were primarily EGFR mutant for del19, with very low wild-type EGFR expression (Fig. 4*B*). Both L858R and the T790M de novo mutations were also detected via our integrated nanoplatform, revealing the heterozygous expression of both mutant and wild-type alleles (Fig. 4 *C*–*F*). We further examined expression levels of EGFR mutations and their corresponding wild-type genes in CTCs from seven advanced NSCLC patients with known mutational statuses. Each putative CTC was identified by EGFR and *TERT* expression, and heterogeneous levels of EGFR expression across those CTCs were observed (Fig. 4*G*).

Assay Performance Comparison. As shown in Fig. S4, bulk PCR measurements performed directly on patients' whole blood yielded undetectable signals for EGFR mutations (del19 and others). Although EGFR wild type was found to be widely expressed from bulk assays of advanced-stage patients' blood, EGFR mutant genes were not. In addition, we assessed the analytical sensitivity of conventional PCR in vitro on NSCLC cell lines (HCC827 and H1650). Our data indicate that, although conventional PCR can reliably detect CTC-specific genes from a total of 100 cancer cells, this signal fluctuates significantly for 10 cells and is undetectable above background for <10 cells. Genes that were insufficiently expressed (e.g., *ALDH*, as in Fig. S5) were not detectable above threshold for samples of 10 or fewer cells. We also note that these experiments were performed on homogenized cell populations to extrapolate the number of cells in a sample, so this approach is expected to yield the most consistent and reliable serial dilution measurements. These observations confirm that conventional PCR cannot reliably assay "enriched" samples of cell populations of <10 or fewer cells, and hence a higher sensitivity approach is needed to reliably assay heterogeneous CTC populations for tumor-specific and therapy-relevant mutant gene panels.

To investigate mutational detection directly from enriched CTC population, we performed (*i*) a conventional PCR on extracted

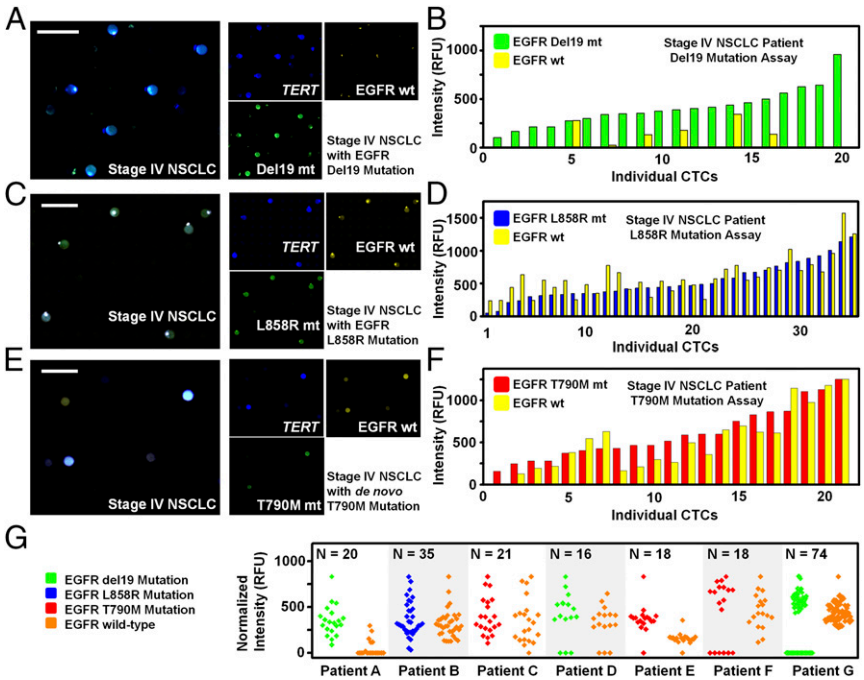

Fig. 4. Multigene expression of CTCs from NSCLC patient blood samples (results from three of the seven patient samples that were analyzed for CTC gene mutation profiling are shown here). (*A*) Mutation detection assay on a stage IV NSCLC patient sample with EGFR del19 mutation previously confirmed by primary tumor biopsy and sequencing. Using a three-plex assay of *TERT* (Cy5, shown in blue), EGFR E746-A750del (FAM, shown in green), and EGFR wild type (HEX, shown in yellow), putative CTCs were identified by high *TERT* expression. (Scale bar, 50 μm.) (*B*) All *TERT*-positive wells (blue) exhibited EGFR mutant signal (green) and very low EGFR wild-type signal (yellow), indicating that putative CTCs were detected and identified as primarily EGFR del19 mutant. Subsequent quantitative analysis of *TERT*-positive wells confirmed the majority of identified putative CTCs were primarily EGFR del19 mutant. In addition, a few putative CTCs also exhibited some EGFR wild-type signal. (*C*) Nanowell scan of the EGFR L858R mutation assay on a stage IV NSCLC patient sample with EGFR L858R mutation. (*D*) Putative CTCs identified by their *TERT* expression exhibit heterozygous expression of both mutant and wild-type forms. (*E*) Nanowell scan of the EGFR T790M mutation assay of a stage IV NSCLC patient sample with de novo EGFR T790M mutation. (*F*) Putative CTCs demonstrate heterozygosity for the mutation. (*G*) Expression levels of EGFR mutations and their corresponding wild-type genes in CTCs from seven advanced NSCLC patients. Each CTC was identified by EGFR and *TERT* expression. Although heterogeneous levels of CTCs and patterns of EGFR expression across those CTCs were observed, follow-up work regarding these patients' clinical outcomes is necessary for proper heterogeneity analysis.

mRNAs from whole-blood samples of three advanced stage NSCLC patients, (*ii*) a conventional PCR on enriched CTCs by the MagSifter technology, and 3) our proposed MagSifter–Nanowell assay in a parallel manner, to compare their sensitivity. mRNAs from whole blood and from enriched CTCs were extracted using the TRIzol protocol described above. Two advanced-stage NSCLC patients with the EGFR del19 mutation, and an advanced-stage NSCLC patient with the EGFR T790M mutation were recruited for assay comparison. In all cases of mRNA analysis from whole blood and enriched CTCs, neither mutant genes (EGFR del19, and EGFR T790M) nor *TERT* were detected (Fig. S5), whereas Nanowell could identify putative CTCs, which are either EGFR mutant, EGFR wild type, or both. This result agrees with our cell line experiment indicated above, thus showing the greater sensitivity of the Nanowell assay, especially when fewer numbers of CTCs are presented.

Additionally, to investigate Nanowell's performance against ICC, we recruited 11 NSCLC patients and 1 healthy donor to directly compare the signal positivity for immunostaining (CK^+, $DAPI^+$, and $CD45^-$) and Nanowell RT-PCR assay ($TERT^+$ and MET^+) (Table S2). Each patient's sample was split into two 2-mL samples for CTC assessment by both conventional enumeration (immunostaining) and Nanowell assay. Note that each 2 mL of patient blood was processed with MagSifter in parallel. Representative immunostained CTCs are illustrated in Fig. S2. All resulting immunostained CTCs were confirmed by a Stanford Hospital pathologist. Enumeration results were positive for 3 of 11 cases (defined as CTC > 1), whereas the Nanowell assay measured positive signals above threshold for 8 of 11 cases, as shown in Table 1 (the full analysis is given in Table S2). These observations indicate the higher sensitivity of our approach, which is because of the signal amplification by PCR. We note that the 11 patients enrolled in this study spanned all lung cancer stages, representing early-stage tumors that are thought to release low numbers of CTCs and those more advanced tumors that are expected to release more CTCs.

Discussion

Our integrated nanoplatform is a high-throughput, massively parallel CTC enrichment and subsequent molecular characterization tool for tumor biology and, potentially, for clinical use as a diagnostic/prognostic tool (38). It achieves accurate identification of hundreds to thousands of putative CTCs with multiplex gene mutation profiling capabilities. Each of the 25,600 nanowell compartments are $20 \times 20 \times 50\ \mu m^3$, with 20-pL volumes that are 10^6 times smaller than those of typical PCR assays, thereby enabling higher sensitivity from higher mRNA concentrations. To this point, we observed that conventional RT-PCR assays of mRNA extracted from patients' blood yielded undetectable *TERT* expression for all samples and no *MET* expression for 76% of patient samples (Fig. S4). Nanowell assays also achieve excellent specificity by using hydrolysis probes (e.g., TaqMan).

Detection of EGFR mutations, such as del19, L858R, and T790M, in lung cancer is now proving critical to inform clinical treatment decisions with EGFR tyrosine kinase inhibitor (TKI) therapies (39). Because 15% of lung adenocarcinomas harbor EGFR mutations—a number that is at least twice as high in the Asian population—many patients undergoing treatment in clinics for whom biopsy material is difficult to obtain may not be receiving optimal therapy. Furthermore, because resistance inevitably develops in patient with EGFR driver mutations that are treated over 12–24 months, and currently this can be monitored only by imaging and clinical gestalt, blood biomarkers for disease monitoring are desperately needed to guide management. Circulating tumor DNA (ctDNA) is a promising avenue to guide therapy, but recent data suggest that CTCs may be a complementary, rather than extraneous, approach (40). For example, ctDNA analysis from a del19 patient (Fig. 4*A*) using cancer personalized profiling by deep sequencing (41) (CaPP-Seq) detected del19 mutation at an allele frequency of 3.12%, indicating nontrivial tumor burden with this particular mutation.

Additionally, recent studies have demonstrated the promising potential of next-generation sequencing (NGS) profiling of CTCs (29, 42), especially to inform prognostic assessment and precise personalized cancer treatment (43). Unfortunately, widespread adoption of NGS for single-CTC sequencing is currently hindered by high costs and technical complexity for extracting clinically actionable information. Our integrated nanoplatform has the advantages of lower cost (with reagent costs of ~25 US dollars per assay) and fast sample-to-answer time (Table S3) given its targeted strategy. Nonetheless, we believe NGS is a powerful tool that will become more cost-effective over time, and we envision using the Nanowell as a validation tool to confirm targets on CTCs discovered by whole-genome approaches.

The modular nature of our multiplex assay using "off-the-shelf" commercial reagents provides versatility for exploring research questions on individual CTCs and acts as a valuable tool for CTC analysis. As an example, we have demonstrated heterogeneous expression of *ALDH* and *VIM* on putative CTCs in this study. Cell immortality and plasticity defined by these types of expression markers are well established to be important in cancer progression. Exactly how this type of CTC heterogeneity affects patient outcome and relates to imaging and clinical parameters is an important, and incipient, avenue of inquiry that should be pursued by research laboratories in the field.

The technology reported here requires further optimization before widespread application in clinical settings. First, comprehensive enrichment of an entire population of heterogeneous CTCs requires the use of multiple capture antibodies. Although our platform currently relies on EpCAM enrichment, the Nanowell assay is highly sensitive and specific to tumor-derived cells neglected by ICC (Fig. S2). Moreover, MagSifter can be generalized to accommodate multiple cell capture antibodies instead of, or in conjunction with, EpCAM. This approach would broaden the platform's utility to many other cancers that shed CTCs [e.g., human epidermal growth factor receptor (HER2) for breast cancer, neuron-glial antigen 2 (NG2) for melanoma, and carbonic anhydrase IX (CAIX) for renal cell carcinoma] and to EpCAM-low and EpCAM-negative populations. Second, our platform currently employs up to four fluorophores for multiplex single-cell gene expression profiling, because primer–probe sets are only commercially available in four discrete excitation–emission spectra that can be resolved by conventional fluorescence microscopy. However, further modifications, including

Table 1. Comparison of putative CTCs assayed by Nanowell (both *TERT* and *MET* positivity) and conventional ICC

Patient ID	Nanowell	ICC	Types	Lung cancer stage
1	39	0	NSCLC	I
2	21	4	NSCLC	II
3	15	1	NSCLC	I
4	14	6	NSCLC	I
5	11	0	NSCLC	III
6	9	0	NSCLC	II
7	9	0	NSCLC	I
8	9	0	NSCLC	IV
9	7	0	NSCLC	I
10	7	7	NSCLC	IV
11	7	0	NSCLC	II
12	0	0	Healthy	N/A

Markedly, the Nanowell assay's analytical sensitivity exceeded that of conventional ICC for putative CTC detection in NSCLC patients. More information can be found in Table S2.

laser excitation, sharper bandpass filters, and narrower-emission hydrolysis probes, may extend the platform's multiplex capability to accommodate 12 or more genes (26). This expansion will allow comprehensive mutational profiling to develop along with clinical advances to capture a comprehensive panel of relevant "actionable" mutations for therapy selection and disease monitoring. We also envision that the Nanowell as a clinical research tool to study (*i*) the assessment of heterogeneity across CTCs with patient's clinical outcomes, (*ii*) lineage mapping studies of biopsied primary tumor cells, (*iii*) correlation studies with cell-free and ctDNA, and (*iv*) discrimination between benign and malignant states for early cancer detection.

Materials and Methods

Patient Samples and Clinical Data. All patient-related research was approved by the Stanford Institutional Review Board before study initiation and informed consent was obtained from the participants. For each patient, samples of whole blood were drawn into 10-mL Vacutainer K_2-EDTA tubes (Becton Dickinson), and sample ID numbers were assigned to anonymize clinical identification. Healthy human blood samples were obtained from the Stanford Blood Center (Palo Alto, CA), and patient blood samples were drawn from those with NSCLC from Pulmonary, Medical Oncology, and Radiation Oncology Clinics at Stanford University Medical Center. Healthy donor samples were used for our spike-in experiments with cell lines and as negative controls, whereas patient blood samples were processed for CTC identification and mutation detection. Lung cancer diagnoses were extracted from the medical record, and we defined advanced-stage NSCLC here as stage IV by the American Joint Committee on Cancer (AJCC-7) staging criteria.

Some NSCLC patient samples were plasma depleted for other research purposes and then resuspended with an equal volume of 1× Gibco PBS buffer (Life Technologies). All blood samples were processed as soon as possible after blood draw (within 1–24 h). For each 7.5-mL blood sample, 2 mL was processed with the MagSifter and ICC for CTC enumeration, 2 mL was independently processed with the integrated nanoplatform for single-CTC gene expression and mutation analysis, and the remaining volume was allocated for total mRNA extraction via a TRIzol protocol for bulk gene expression analysis.

Nanowell Processing. Following CTC enrichment by MagSifter and treatment of the eluent with lysis buffer and DNase, the entire eluent was loaded into an assembled Nanowell array (Fig. S1*D*), by centrifugation at 3,000 rpm for 10 min. Because each Nanowell array contains 25,600 wells and the CTC population from 2 mL of blood is expected to be no more than 2,000 cells, each individual well has a 99.7% chance of containing either a single cell or no cell, according to the Poisson distribution (Table S4), and only a 0.3% of containing two or more cells, thereby representing a high-throughput method of analyzing "single" cells. Identification of putative CTCs was then performed as follows. First, fluorescence microscope images of the entire Nanowell array were acquired for identification and exclusion of wells containing WBCs by CD45 signal. Next, the entire Nanowell array was completely dried at 70 °C for 10 min to fix seeded cells into the wells and to completely deactivate the DNase. Then, an RT-PCR master mix was applied, and the array was centrifuged for nanowell seeding at 3,000 rpm (Sorvale Legend RT Centrifuge; Thermo Fisher Scientific) for 10 min. The RT-PCR master mix consisted of 2× reaction mix (CellsDirect One-Step qRT-PCR; Life Technologies), polymerases (SuperScript III RT/Platinum Taq Mix; Life Technologies), TaqMan probes (Life Technologies; Bio-Rad) for targeting specific genes, and diethylpyrocarbonate (DEPC)-treated water (for detailed quantities, see Table S5). To prevent water evaporation during PCR thermocycling, the array was then capped with a small piece of adhesive PCR sealant film (Bio-Rad) and centrifuged at 3,000 rpm for 10 min, and white mineral oil (W. S. Dodge Oil) was applied around the array edges. The array was then loaded into a thermal cycler (PTC-200; Peltier Thermal Cycler; Bio-Rad) using the following cycle parameters: for the first thermal cycler step, cell lysis and subsequent reverse transcription, the array was incubated at 50 °C for 45 min. This was followed by 10 cycles of 60 s at 95 °C for denaturation and 90 s at 65 °C for an annealing and extension step. Amplification commenced after with 35 cycles of 60 s at 90 °C and 90 s at 60 °C.

Nanowell Signal Acquisition. For all Nanowell assays, automated scanning of the full array was performed at Stanford University's Cell Science Imaging Facility (CSIF) on a Zeiss Axio Imager fluorescence microscope (Carl Zeiss) with Zeiss ZEN Pro software. Each Nanowell was imaged for FAM, HEX, Texas Red, and Cy5 fluorescence after single-cell RT-PCR with a ZEISS Axiocam 503 monochrome camera. For each Nanowell, 100 regions of the array were imaged at 10× magnification, and images were stitched together with ZEN Pro software.

Marker Gene and Fluorophore Selection. We reviewed the biomedical literature using the search terms "circulating tumor cell," "lung cancer," and "blood" in MEDLINE to identify potential biomarkers for single-cell expression analysis of CTCs. We identified about 400 articles pertaining to lung cancer CTCs, and from this literature, we identified *TERT* (29, 30, 44–48) and *MET* (31, 32, 49–52) as promising marker genes for the CTC identification panel. *TERT* is up-regulated by many oncogenes, and overexpression of *TERT* is well established as dysregulated in cancers. *TERT* is required for the perpetuation of the malignant clone during cancer progression as it elongates telomeres in each cell division, but is not expressed in normal somatic cells. Similarly, hepatocyte growth factor receptor (HGFR), or *MET*, is a proto-oncogene whose up-regulation is closely associated with NSCLC. Similarly, we reviewed the literature and identified *VIM* and *ALDH* as promising marker genes for the heterogeneity panel. *VIM* is an epithelial–mesenchymal transition (EMT) marker, whose expression indicates the increased potential for tumor metastasis (36). Multiple markers of cancer cell stemness exist, but we chose *ALDH* as a marker that indicates tumorigenicity and clonogenicity of lung cancer (37) based on commercially available primer–probe sets. Finally, for the therapy prediction and monitoring panel, we selected EGFR E746-A750del mutation, its associated wild-type gene, and *TERT*. Other clinically relevant EGFR mutations, including L858R and T790M, can also be included as needed. Each marker was assigned a specific fluorescence channel: FAM (492-nm excitation, 517-nm emission) to *TERT*, HEX (530-nm excitation, 556-nm emission) to *MET*, Texas Red (596-nm excitation, 615-nm emission) to *VIM*, and Cy5 (650-nm excitation, 670-nm emission) to *ALDH*.

Four-Gene Expression Development. Simultaneous gene expression measurement of two genes in the Nanowell array was previously reported (26). To extend this capability to accommodate four-plex gene expression analysis on a single cell, the procedure was optimized to avoid issues of reagent depletion and weaker signal for lower-expressing genes (53). We selected probes with four different fluorophores and minimal spectral overlap for simultaneous four-plex gene expression capability. The four fluorophores, FAM, HEX, Texas Red, and Cy5, had excitation and emission peaks of 492 and 517 nm, 530 and 556 nm, 596 and 615 nm, and 650 and 670 nm, respectively. Primer–probe assays were obtained commercially: *TERT* (Life Technologies), *MET* (Life Technologies), *VIM* (Bio-Rad), and *ALDH* (Bio-Rad). The four-plex RT-PCR process was optimized on conventional bulk assay in a CFX96 Touch Real-Time PCR Detection System (Bio-Rad).

Statistical Analysis. After single-cell RT-PCR and fluorescence image acquisition were performed, custom-developed MATLAB and R scripts were used to analyze signals from the Nanowell arrays. For the diagnosis of NSCLC patients with Nanowell assays for *TERT* and *MET*, the following protocol was performed. Bright-field images acquired before and after single-cell RT-PCR were first manually inspected for the pixel locations of the Nanowell array at the top left, top right, and bottom left of the image area to be analyzed. These pixel locations were entered into a MATLAB script that extracted the pixel spacing information for the Nanowell array by using its natural periodicity. The script then used this periodicity to extrapolate the location of each nanowell within the image area of interest, and extracted the pixel intensities within each nanowell for every fluorescence channel of interest. As successful amplification in a nanowell results in an extremely bright spot within the nanowell, it was determined that a metric comparing the dispersion of pixel intensities within each nanowell could determine whether amplification had successfully occurred. Thus, a custom R script was used to run an outlier detection algorithm for each fluorescence image, whereby a z score for the variance in pixel intensity within each nanowell was computed to determine the probability of each individual point being an outlier from the entire population. Due to the large number of nanowells in each population (typically >5,000 per image analyzed), the central limit theorem dictates that the distribution should follow a normal distribution, thus allowing use of the Z test to identify outliers at a significance level of $P < 0.05$. Additionally, due to the large number of points tested per image, Bonferroni correction was performed when conducting the Z test to avoid excessive type I errors, with the Bonferroni correction commonly regarded as one of the most conservative ways to control familywise error rates. The R script then computed a count for the nanowells with z scores above this threshold and classifies these nanowells as positive for the particular measurement. The images in the individual fluorescence channels were analyzed separately, and the nanowell counts were then collated either individually (as in the PE-fluorescence image pre–RT-PCR when excluding nanowells with WBCs) or together (as per the use of both FAM and HEX channel images when

enumerating potentially cancerous entities after RT-PCR). For all analysis of images acquired by the Zeiss Axio Imager, including the EGFR mutation assay and the four-marker gene expression panel, individual nanowell fluorescence intensities were extracted from ZEN Pro for each channel and collated manually after subtraction of background intensities from the empty nanowells.

Identification of Putative CTCs. In this study, "putative CTCs" are mostly defined as cells with the multigene signature having high expression in both *TERT* and *MET* genes. This multigene approach yields the best assay performance (compared with a single-gene assay of either *TERT* or *MET*) by minimizing the frequency of "false positives" that are acquired because of intrinsic and extrinsic sources of background noise. In addition, for mutational detection purposes, we define putative CTCs as cells having either *TERT* and an EGFR mutation gene, or *TERT* and the corresponding EGFR wild-type gene. Transcriptomic profiles of putative CTCs are stable up to 12 hours from the blood draw (Fig. S6).

ACKNOWLEDGMENTS. We thank Dr. Pragya Tripathi for assistance with preparation of patient blood samples, Dr. Ivan K. Dimov and Prof. Aram J. Chung for helpful discussions, and Dr. Christopher M. Earhart for MagSifter fabrication expertise. We also thank the Stanford Nanofabrication Facility for use of nanofabrication tools, the Cell Science Imaging Facility (CSIF) at Stanford for use of a Zeiss Axio Imager fluorescence camera, and the Lurie Nanofabrication Facility at University of Michigan (Ann Arbor, MI) for contributing to the MagSifter fabrication. This research was supported by NIH Awards U54CA151459 (to the Center for Cancer Nanotechnology Excellence and Translation) and R21CA185804 (to S.S.G. and S.X.W.), the Canary Foundation (S.S.G. and V.S.N.), and the LUNGevity Foundation (V.S.N.).

1. Hanash SM, Baik CS, Kallioniemi O (2011) Emerging molecular biomarkers—blood-based strategies to detect and monitor cancer. *Nat Rev Clin Oncol* 8(3):142–150.
2. Krebs MG, et al. (2014) Molecular analysis of circulating tumour cells—biology and biomarkers. *Nat Rev Clin Oncol* 11(3):129–144.
3. Tibbe AG, et al. (1999) Optical tracking and detection of immunomagnetically selected and aligned cells. *Nat Biotechnol* 17(12):1210–1213.
4. Nagrath S, et al. (2007) Isolation of rare circulating tumour cells in cancer patients by microchip technology. *Nature* 450(7173):1235–1239.
5. Stott SL, et al. (2010) Isolation of circulating tumor cells using a microvortex-generating herringbone-chip. *Proc Natl Acad Sci USA* 107(43):18392–18397.
6. Castro CM, et al. (2014) Miniaturized nuclear magnetic resonance platform for detection and profiling of circulating tumor cells. *Lab Chip* 14(1):14–23.
7. Talasaz AH, et al. (2009) Isolating highly enriched populations of circulating epithelial cells and other rare cells from blood using a magnetic sweeper device. *Proc Natl Acad Sci USA* 106(10):3970–3975.
8. Earhart CM, et al. (2014) Isolation and mutational analysis of circulating tumor cells from lung cancer patients with magnetic sifters and biochips. *Lab Chip* 14(1):78–88.
9. Sarioglu AF, et al. (2015) A microfluidic device for label-free, physical capture of circulating tumor cell clusters. *Nat Methods* 12(7):685–691.
10. Krebs MG, et al. (2012) Analysis of circulating tumor cells in patients with non-small cell lung cancer using epithelial marker-dependent and -independent approaches. *J Thorac Oncol* 7(2):306–315.
11. Sollier E, et al. (2014) Size-selective collection of circulating tumor cells using Vortex technology. *Lab Chip* 14(1):63–77.
12. Ozkumur E, et al. (2013) Inertial focusing for tumor antigen-dependent and -independent sorting of rare circulating tumor cells. *Sci Transl Med* 5(179):179ra47.
13. Li W, et al. (2015) Biodegradable nano-films for capture and non-invasive release of circulating tumor cells. *Biomaterials* 65:93–102.
14. Lin M, et al. (2014) Nanostructure embedded microchips for detection, isolation, and characterization of circulating tumor cells. *Acc Chem Res* 47(10):2941–2950.
15. Yoon HJ, et al. (2013) Sensitive capture of circulating tumour cells by functionalized graphene oxide nanosheets. *Nat Nanotechnol* 8(10):735–741.
16. Marrinucci D, et al. (2012) Fluid biopsy in patients with metastatic prostate, pancreatic and breast cancers. *Phys Biol* 9(1):016003.
17. Maheswaran S, et al. (2008) Detection of mutations in EGFR in circulating lung-cancer cells. *N Engl J Med* 359(4):366–377.
18. Devriese LA, et al. (2012) Circulating tumor cell detection in advanced non-small cell lung cancer patients by multi-marker QPCR analysis. *Lung Cancer* 75(2):242–247.
19. Sieuwerts AM, et al. (2009) Molecular characterization of circulating tumor cells in large quantities of contaminating leukocytes by a multiplex real-time PCR. *Breast Cancer Res Treat* 118(3):455–468.
20. Haber DA, Velculescu VE (2014) Blood-based analyses of cancer: Circulating tumor cells and circulating tumor DNA. *Cancer Discov* 4(6):650–661.
21. Powell AA, et al. (2012) Single cell profiling of circulating tumor cells: Transcriptional heterogeneity and diversity from breast cancer cell lines. *PLoS One* 7(5):e33788.
22. Chen CL, et al. (2013) Single-cell analysis of circulating tumor cells identifies cumulative expression patterns of EMT-related genes in metastatic prostate cancer. *Prostate* 73(8):813–826.
23. Jemal A, et al. (2011) Global cancer statistics. *CA Cancer J Clin* 61(2):69–90.
24. Shepherd FA, et al.; National Cancer Institute of Canada Clinical Trials Group (2005) Erlotinib in previously treated non-small-cell lung cancer. *N Engl J Med* 353(2):123–132.
25. Solomon BJ, et al.; PROFILE 1014 Investigators (2014) First-line crizotinib versus chemotherapy in ALK-positive lung cancer. *N Engl J Med* 371(23):2167–2177.
26. Dimov IK, et al. (2014) Discriminating cellular heterogeneity using microwell-based RNA cytometry. *Nat Commun* 5:3451.
27. Park SM, et al. (2016) Dual transcript and protein quantification in a massive single cell array. *Lab Chip* 16(19):3682–3688.
28. Al-Soud WA, Rådström P (2001) Purification and characterization of PCR-inhibitory components in blood cells. *J Clin Microbiol* 39(2):485–493.
29. Ni X, et al. (2013) Reproducible copy number variation patterns among single circulating tumor cells of lung cancer patients. *Proc Natl Acad Sci USA* 110(52):21083–21088.
30. Sozzi G, et al. (2003) Quantification of free circulating DNA as a diagnostic marker in lung cancer. *J Clin Oncol* 21(21):3902–3908.
31. Kubo T, et al. (2009) MET gene amplification or EGFR mutation activate MET in lung cancers untreated with EGFR tyrosine kinase inhibitors. *Int J Cancer* 124(8):1778–1784.
32. Tsao M-S, et al. (1993) Hepatocyte growth factor/scatter factor is an autocrine factor for human normal bronchial epithelial and lung carcinoma cells. *Cell Growth Differ* 4(7):571–579.
33. Kato Y, et al. (2010) Novel epidermal growth factor receptor mutation-specific antibodies for non-small cell lung cancer: Immunohistochemistry as a possible screening method for epidermal growth factor receptor mutations. *J Thorac Oncol* 5(10):1551–1558.
34. Satelli A, et al. (2014) Universal marker and detection tool for human sarcoma circulating tumor cells. *Cancer Res* 74(6):1645–1650.
35. Krebs MG, et al. (2011) Evaluation and prognostic significance of circulating tumor cells in patients with non-small-cell lung cancer. *J Clin Oncol* 29(12):1556–1563.
36. Al-Saad S, et al. (2008) The prognostic impact of NF-kappaB p105, vimentin, E-cadherin and Par6 expression in epithelial and stromal compartment in non-small-cell lung cancer. *Br J Cancer* 99(9):1476–1483.
37. Jiang F, et al. (2009) Aldehyde dehydrogenase 1 is a tumor stem cell-associated marker in lung cancer. *Mol Cancer Res* 7(3):330–338.
38. Park SM, Sabour AF, Son JH, Lee SH, Lee LP (2014) Toward integrated molecular diagnostic system (*i*MDx): Principles and applications. *IEEE Trans Biomed Eng* 61(5):1506–1521.
39. Kobayashi S, et al. (2005) EGFR mutation and resistance of non-small-cell lung cancer to gefitinib. *N Engl J Med* 352(8):786–792.
40. Sundaresan TK, et al. (2016) Detection of T790M, the acquired resistance EGFR mutation, by tumor biopsy versus noninvasive blood-based analyses. *Clin Cancer Res* 22(5):1103–1110.
41. Newman AM, et al. (2014) An ultrasensitive method for quantitating circulating tumor DNA with broad patient coverage. *Nat Med* 20(5):548–554.
42. Ramsköld D, et al. (2012) Full-length mRNA-Seq from single-cell levels of RNA and individual circulating tumor cells. *Nat Biotechnol* 30(8):777–782.
43. Lohr JG, et al. (2014) Whole-exome sequencing of circulating tumor cells provides a window into metastatic prostate cancer. *Nat Biotechnol* 32(5):479–484.
44. Miyazu YM, et al. (2005) Telomerase expression in noncancerous bronchial epithelia is a possible marker of early development of lung cancer. *Cancer Res* 65(21):9623–9627.
45. Lantuejoul S, et al. (2004) Differential expression of telomerase reverse transcriptase (hTERT) in lung tumours. *Br J Cancer* 90(6):1222–1229.
46. Zhu CQ, et al. (2006) Amplification of telomerase (hTERT) gene is a poor prognostic marker in non-small-cell lung cancer. *Br J Cancer* 94(10):1452–1459.
47. Fujita Y, et al. (2003) The diagnostic and prognostic relevance of human telomerase reverse transcriptase mRNA expression detected in situ in patients with nonsmall cell lung carcinoma. *Cancer* 98(5):1008–1013.
48. Miura N, et al. (2006) Clinical usefulness of serum telomerase reverse transcriptase (hTERT) mRNA and epidermal growth factor receptor (EGFR) mRNA as a novel tumor marker for lung cancer. *Cancer Sci* 97(12):1366–1373.
49. Tsao M-S, et al. (1998) Differential expression of Met/hepatocyte growth factor receptor in subtypes of non-small cell lung cancers. *Lung Cancer* 20(1):1–16.
50. Sierra JR, Tsao M-S (2011) c-MET as a potential therapeutic target and biomarker in cancer. *Ther Adv Med Oncol* 3(1, Suppl):S21–S35.
51. Sheu C-C, et al. (2006) Combined detection of CEA, CK-19 and c-met mRNAs in peripheral blood: A highly sensitive panel for potential molecular diagnosis of non-small cell lung cancer. *Oncology* 70(3):203–211.
52. Cheng T-L, et al. (2005) Overexpression of circulating c-met messenger RNA is significantly correlated with nodal stage and early recurrence in non-small cell lung cancer. *Chest* 128(3):1453–1460.
53. Henegariu O, Heerema NA, Dlouhy SR, Vance GH, Vogt PH (1997) Multiplex PCR: Critical parameters and step-by-step protocol. *Biotechniques* 23(3):504–511.
54. Earhart CM, Wilson RJ, White RL, Pourmand N, Wang SX (2009) Microfabricated magnetic sifter for high-throughput and high-gradient magnetic separation. *J Magn Magn Mater* 321(10):1436–1439.
55. Yu M, et al. (2012) RNA sequencing of pancreatic circulating tumour cells implicates WNT signalling in metastasis. *Nature* 487(7408):510–513.
56. Lustberg M, Jatana KR, Zborowski M, Chalmers JJ (2012) Emerging technologies for CTC detection based on depletion of normal cells. *Recent Results Cancer Res* 195:97–110.